

Chapter 7

Soft Ferromagnetic Microwires with Excellent Inductive Heating Properties for Clinical Hyperthermia Applications

Rupin Singh, Javier Alonso, Jagannath Devkota, and Manh-Huong Phan

7.1 Introduction

7.1.1 Overview

Although the spread of cancer continues to decline, down twenty-two percent in the USA over the past two decades [1], it is still the leading cause of death worldwide, accounting for 8.2 million deaths in 2012 alone [2]. Therefore, there is a pressing need to improve and develop cancer treatments to continue to improve survival rates and patient well-being. The unregulated growth of cells associated with cancer normally causes a low pH and hypoxia to occur in the tumors and surrounding tissue [3]. These are not ideal conditions for radiation therapy or cytotoxic drugs as their delivery is severely hindered to a much lower concentration. Additional treatment cannot be done without doing harm to the patient as well, such as inducing high levels of radiation to patients. Magnetic hyperthermia is one alternative avenue researchers are investigating to improve cancer treatments success rates and reduce patient discomfort.

The use of magnetic nanoparticles in medicine is rapidly growing due to their variability in size, shape, coating, and ability to perform noninvasive procedures. They can be used as a means to monitor chemical and biological systems as magnetic sensors, to perform deep tissue penetration for drug delivery, magnetic cell separation and purification, magnetic resonance imaging contrast enhancement,

R. Singh • J. Devkota • M.-H. Phan (✉)

Department of Physics, University of South Florida, Tampa, FL 33620, USA
e-mail: rupin@mail.usf.edu; jagan.devkota@gmail.com; phanm@usf.edu

J. Alonso

Department of Physics, University of South Florida, Tampa, FL 33620, USA

BCMaterias Edificio No. 500, Parque Tecnológico de Vizcaya, Derio 48160, Spain
e-mail: jalansomasa@gmail.com

purification, bioassay, gene transfer, and hyperthermia of cancerous tissue [4–6]. For magnetic hyperthermia, however, magnetic nanoparticles present some limitations. It has been reported that if the nanoparticles are injected intravenously they tend to be covered with proteins (opsonized), thus encouraging their phagocytosis. The nanoparticles can also be recognized as “foreign bodies” and eliminated by the reticuloendothelial system [7]. To avoid the action of the immune system, there is an increasing need for controlling their size, surface functionality, aggregation, and size distribution. It has also been reported that once the treatment is finished, the nanoparticles tend to accumulate in the liver and spleen, with possibly unwanted toxic effects [8]. Therefore, alternative materials have recently been proposed. In particular, the use of ferromagnetic implants or needles for magnetic hyperthermia, which was recognized a few decades ago as a promising approach [9], has brought renewed interest in the scientific community [10].

Soft ferromagnetic glass-coated microwires (GCMWs) of 5–150 μm diameter have emerged as one of the most promising soft magnetic materials, owing to their outstanding magnetic properties (e.g., magnetic bistability, giant magneto-impedance (GMI) effect, fast domain wall propagation, and Hopkinson effect) for a wide variety of applications in magnetic sensors, microelectronics, security, and biomedical engineering [10–14]. The continuous microwires up to few kilometers can easily be fabricated from 1 gram of master alloy [11]. The extremely large saturation magnetization and shape anisotropy coupled with their strong responses to AC magnetic fields suggest that the GCMWs can be a promising candidate for use in magnetic hyperthermia. The glass coating itself provides electrical insulation and also improves biocompatibility [14].

In this study, we aim to explore radio frequency field responses of magnetically soft Co-rich glass-coated microwires for clinical hyperthermia applications while investigating the effect of multiple variables of interest including metal composition, core diameter, glass-coating diameter, orientation, and multiple microwire interactions.

7.1.2 Magnetic Hyperthermia

Magnetic hyperthermia mediated by magnetic structures is based on raising the temperature of a localized tumor area in order to impede or kill malignant cells within the body. Normally performed synergistically with more common treatments such as radiotherapy and chemotherapy [3, 6, 15], hyperthermia is usually carried out at defined local hyperthermic levels, i.e., temperatures around 42–45 °C. In this temperature range, hyperthermia does not induce cell death, only disrupts cellular metabolism, and impedes cancer proliferation. On the other hand, thermoablation relies on the use of hyperthermia in order to induce rapid cell death at temperatures above 50 °C. At this point, vital proteins of the cancer cell become damaged and the cell membrane partially dissolves into the aqueous solution surrounding it [15]. This technique has a high risk of severe or persistent side-effects and can potentially lead to dire consequences depending on the size of

the target region. Thermoablation may be feasible for some cancer morphologies but as long as one can assure side-effects are reduced to reasonable levels.

The basic magnetic hyperthermia involves injecting a ferrofluid, i.e., a stable colloidal dispersion of iron magnetic particles in an aqueous media, or inserting wires into the cancerous body [3, 6]. The cancerous location in the body is remotely targeted from active or passive external magnetic field gradients and then subsequently an external alternating magnetic field (usually between a few kHz to 1 MHz) is applied to the localized site in order to heat cancer cells. Contemporary research demonstrates an ability to increase specificity and reliability of magnetic structures for hyperthermia by altering delivery methods, synthesis methods, optimization of their coating, optimization of their size to heat delivered ratio, and attempts to reduce the indirect heating of healthy tissue [16].

The use of fine magnetic particles for magnetic hyperthermia has not only been known for decades but also has been an active field of research for over 50 years [10]. Early research by Dr. Gilchrist was first done in 1965 to kill lymph node metastases [17]. It was an attempt to treat colon cancer by applying an alternating magnetic field of 55 kHz to the ferrite nanoparticles of size 100–500 nm. Gilchrist demonstrated that by applying an external AC field, the nanoparticles gave rise to heat losses proportional to the frequency of the field [17]. The targeted tissue is mainly heated by two physical phenomena: eddy currents and magnetic hysteresis [3, 6]. The eddy currents, the primary heat source in typical bulk magnetic structures, oppose the applied magnetic field and by the Joule effect, produce heating [18]. In ferromagnetic materials, such as magnetic particles, the heating is mainly due to magnetic hysteresis losses originated by the lag between the magnetic moments of the particles and the oscillating magnetic field [19]. The advantages of using modern hyperthermia systems are huge and all are important to the patient's safety and well-being.

In addition to the use of fine magnetic particles, ferromagnetic implants, i.e., needles or micro/nanowires, have been developed for enhanced hyperthermia. It has recently been reported that the magnetic needles show even higher heating efficiency rates, as compared to iron oxide nanoparticles [20]. Therefore, it is more important than ever to be able to control the spatial distribution of heat to be both very strong and homogenous. Additionally, ferromagnetic microwires have demonstrated the ability to be self-regulated because of their tailored Curie temperatures [21]. Some materials proposed outside microwires include Fe-based amorphous ribbons, biocompatible Mg-Fe-based ceramics, and nickel-zinc nanoparticles [21].

7.1.3 Soft Ferromagnetic Glass-Coated Microwires

Glass-coated microwires are a composite material that consists of a metallic nucleus and a glass coating. The metallic nucleus ranges from 100 nm to 50 μm in diameter while the glass-coated thickness ranges from 2 to 20 μm [12]. As a result

of their amorphous structure, glass-coated microwires are characterized by low magnetic anisotropy. Their magnetic properties are mainly dictated by magnetoelastic and shape anisotropy. Overall, amorphous microwires possess large shape anisotropy, magnetoelastic anisotropy, and ultra-soft magnetic properties such as a high permeability, large saturation magnetization (M_s), and low magnetic field anisotropy (H_s). They have a characteristic core/shell structure that dictates their magnetic properties [11–13].

Soft ferromagnetic amorphous glass-coated microwires are particularly interesting because thus far their research has been limited to other applications such as GMI and microwave sensing [13, 22, 23]. Their applications in hyperthermia could open a new avenue for biocompatible hyperthermic treatments without the need for carefully crafted magnetic nanoparticles and nanowires. Their commercial availability and cheap/efficient preparation increase the access institutions to have for the treatment which can ultimately lower the cost of care for both the health care provider and the patient. During the production of these amorphous glass-coated microwires, a combination of axial and tensile radial stresses affects their magnetic properties [12, 13]. This is usually dependent on the metallic composition of the alloy causing them to be divided into three groups: positive magnetostrictive, negative magnetostrictive, and low magnetostrictive.

Positive magnetostrictive wires are Fe-rich alloys, negative magnetostrictive wires are Co-rich (mainly CoSiB-based microwires), and low magnetostrictive wires are usually CoFeSiB-based microwires with 3–5 % Fe-based. The domain structures for each of these are shown in Fig. 7.1. It can be seen that amorphous magnetic microwires form a core-shell type of domain structure but in different patterns and orientations depending on their magnetostriction. The positive magnetostrictive microwires have longitudinal core domains oriented along the wire axis while the shell forms radial domains (Fig. 7.1a). Due to this domain structure,

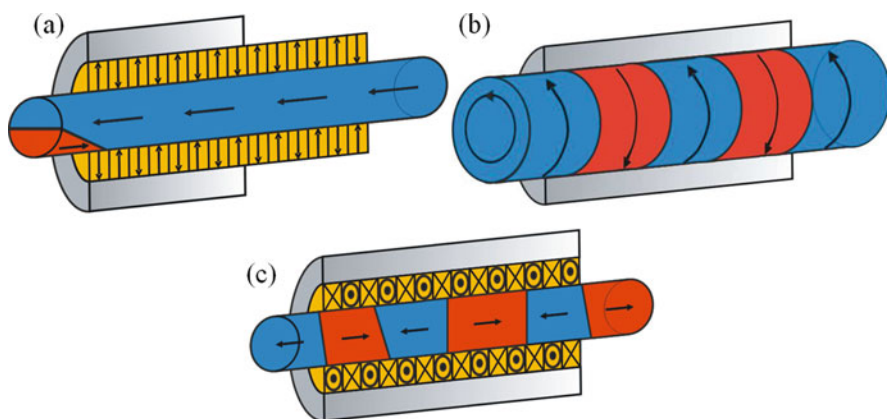


Fig. 7.1 Schematic domain structures of glass-coated microwires with (a) positive magnetostriction, (b) negative magnetostriction, and (c) low magnetostriction. Reprinted with permission from [24]

the magnetization process propagates along the entire microwire in a single Barkhausen jump, forming a rectangular-shaped magnetic hysteresis loop. Due to this, they are easy to detect and are commonly used in the construction of small sensors. Negative magnetostrictive alloys form circular domains perpendicular to the domain axis (Fig. 7.1b). Therefore, magnetization in the axial direction along the microwire causes rotations of magnetic moments inside the domains so their magnetization is proportional to the applied magnetic field.

The hysteresis loops of negative magnetostrictive microwires are small due to the perpendicular alignment of the magnetic moments in an external magnetic field. The low magnetostrictive alloys have less defined domain structures, as visible in Fig. 7.1c, but still show circular domains below the surface of the nucleus and an axial domain in the center of the wire [13]. These nearly zero magnetostrictive microwires demonstrate normal-shaped hysteresis loops due to the balance between the magnetoelastic and magnetostatic energies.

To exhibit an excellent hyperthermic effect, microwires should have extremely soft magnetic properties, large but well-defined anisotropy, and negative magnetostriction [10, 14]. Considering this, we have selected the two following materials for our study, CoMnSiB and CoFeSiBCrNi, both of them exhibiting negative magnetostriction. Once an external magnetic field is applied, the effects of orientation to the magnetic field and interactions between different microwires have been tested to see if the domain structures have a positive or negative effect on the field's effectiveness. In addition, we have also investigated how the thickness of the glass coating and the core diameter affect the hyperthermia efficiency of these microwires. Finally, the effect of having multiple microwires interacting among each other has been analyzed.

7.2 Experimental

7.2.1 Fabrication and Characterization

The Co-rich amorphous glass-coated microwires used in this experiment were fabricated by the Taylor-Ulitovsky technique, a more advanced form of the normal Taylor-wire spinning synthesis [25]. The glass-coated microwires come in two different alloy compositions which we will describe using their manufacturer labels, 1675 and 1597. Both are soft magnetic amorphous Co-rich microwires with complex magnetic characteristics. The composition of each microwire is outlined in Tables 7.1 and 7.2. The tables show that alloy number 1675 is $\text{Co}_{68}\text{B}_{15}\text{Si}_{10}\text{Mn}_7$ and alloy number 1597 is $\text{Co}_{64.61}\text{B}_{16}\text{Si}_{11}\text{Fe}_{4.97}\text{Cr}_{3.4}\text{Ni}_{0.02}$.

These microwires have high curie temperatures and crystallization temperatures, making them ideal for hyperthermia because of their ability to maintain their magnetization properties at high temperatures. For example, the Curie temperature of 1597 is 250 °C and the crystallization temperature is 520 °C. The density of each

Table 7.1 Composition of alloy number 1675

| Metal | Mass (%) | Atomic (%) |
|-------|----------|------------|
| Co | 82.90 | 68.00 |
| B | 3.40 | 15.00 |
| Si | 5.80 | 10.00 |
| Mn | 7.90 | 7.00 |

Table 7.2 Composition of alloy number 1597

| Metal | Mass (%) | Atomic (%) |
|-------|----------|------------|
| Fe | 5.85 | 4.97 |
| Co | 80.26 | 64.61 |
| B | 3.62 | 16.00 |
| Si | 6.48 | 11.00 |
| Cr | 3.76 | 3.40 |
| Ni | 0.02 | 0.02 |

of these microwire alloys was estimated based on their mass percent. The estimation is normally only useful for crystalline alloys rather than amorphous ones but provides good estimation of the true density without physically removing the glass coating and measuring the densities in the lab. The formula used to estimate the density is shown below:

$$\frac{1}{D_f} = \sum_1^n \frac{x_n}{D_n} \quad (7.1)$$

where D_f is the final density of the alloy, n is the number of metals that make up the alloy, x is the mass fraction of that metal in the alloy, and D is the density of the pure metal. The estimated density of alloy 1675 is 6.98 g/cm^3 and the estimated density of alloy 1597 is 6.84 g/cm^3 .

In addition to using two different alloys, wires of different core diameters and glass thicknesses were used to determine how each affects the inductive heating efficiency. As a side-effect of the synthesis technique, the microwires do not have the same diameter across the entire length of the wire. The average diameter, however, has been calculated and is used as the measuring point. Each thickness was given a number label that corresponds to its alloy. #1–4 correspond to alloy number 1675, while #5–12 correspond to alloy number 1597. The average diameters of the total, core, and glass coating for each microwire tested are summarized in Table 7.3.

To further characterize the structural characteristics of these microwires, we employed a combination of X-ray diffractometry (XRD) and scanning electron microscopy (SEM). For XRD, a Bruker AXS D8 diffractometer with $\text{Cu K}\alpha$ 1.5418 Å was used in a θ – 2θ mode in order to get information about crystal phases of the Co-rich microwires. The XRD data gave us information about how amorphous the microwires used in this experiment truly are. On the other hand, a JEOL JSM-6390LV SEM was used to image the surface morphology of the Co-rich

Table 7.3 Average thicknesses of the microwires

| Alloy and label | Total thickness (μm) | Core thickness (μm) | Glass thickness (μm) |
|-----------------|-----------------------------------|----------------------------------|-----------------------------------|
| 1675-1 | 28.8 | 22.8 | 6.0 |
| 1675-2 | 20.2 | 12.9 | 7.3 |
| 1675-3 | 21.7 | 15.6 | 6.1 |
| 1675-4 | 32.5 | 25.3 | 7.2 |
| 1597-7 | 26.9 | 16.9 | 10.0 |
| 1597-8 | 18.2 | 12.7 | 5.5 |
| 1597-10 | 23.4 | 16.5 | 6.9 |
| 1597-11 | 22.7 | 16.7 | 6.0 |
| 1597-12 | 19.8 | 14.2 | 5.6 |

microwires. SEM was only used to image a single microwire as a representative sample to describe the general structure of these microwires including both their glass coating and their inner amorphous metal core.

Finally, the magnetic characterization of the microwires presented in this experiment was performed in a physical property measurement system (PPMS) from Quantum Design with an installed vibrating sample magnetometer probe. The system can measure properties in a temperature range of 2–350 K and induce magnetic fields up to ± 7 T.

7.2.2 Magnetic Hyperthermia

In order to perform the hyperthermia experiments, the Co-rich microwires were cut into 5 mm strands. Multiple different configurations of microwire alloy, diameter, orientation, quantity, and separation were examined. The single microwire examinations were done for alloys number 1675 1–4 and 1597 7, 8, 10, 11, and 12. Alloys number 1675 1–4 were studied for their general differences in microwire diameter as both the core diameter and the glass thickness varied between the four samples. The samples from alloy number 1597 were carefully selected to investigate the effects of core diameter while the glass thickness was held constant and the effects of the glass thickness while the core diameter was held constant. Alloys number 1597 7, 10, and 11 demonstrated the former effect while 1597-8 and 1597-12 demonstrated the latter effect. Additionally, the sample that demonstrated the best heating was used for additional experiments including orientation, i.e., horizontal versus vertical, and the effects of using multiple microwires.

The single microwire samples were prepared by inserting a single microwire of 5 mm in length into a glass vial filled with 1 mL of deionized water. To test for orientation, the single microwire was placed into a 2 % agar solution that would maintain the orientation of the microwire even under high magnetic fields. The orientation was imposed by the use of a small external permanent magnet and physically aligning it in solution before the agar cooled completely. Tests on



Fig. 7.2 Magnetic hyperthermia system employed. Generator on the *left* and radio frequency amplifier on the *right*

multiple microwires were done both in water and in agar. The tests in water would demonstrate natural microwire orientation in movement in a random distribution. On the other hand, the tests in agar were specifically done in different distributions or orientations, i.e., in situations where the wires are together, separated, and horizontal. The microwires in the multiple microwire experiments were also 5 mm in length.

In this experiment, we have used an Ambrell Easyheat system that can generate an alternating magnetic field at a frequency between 150 and 400 kHz. Figure 7.2 shows an image of the water refrigerated multi-turn helical coil connected to a radio frequency power amplifier. Power to the system is provided by a generator. During the hyperthermia experiments, for each sample, the temperature evolution with time has been monitored while applying an external AC field, between 400 and 800 Oe, at a constant frequency of 310 kHz. The temperature was monitored by using a fiber optic temperature probe which automatically recorded the data to the PC.

The heating efficiency, also known as the specific absorption rate (SAR), of the microwires has been estimated following calorimetric methods: the initial slope $\Delta T/\Delta t$ of the sample has been obtained from the measured heating curves, and the SAR values have been derived from the following formula:

$$SAR = C_p \cdot \frac{\Delta T}{\Delta t} \phi \quad (7.2)$$

where ϕ corresponds with the concentration of magnetic material, C_p is the heat capacity of water, and $\Delta T/\Delta t$ is the initial slope. To remove the heating contribution coming from the coil, we have subtracted the slope measured for the vial without sample from all our measurements. The initial slope was taken shortly after heating began, i.e., when the temperature increase was nearly linear.

Due to the small mass of these microwires (10^{-5} g), the final concentration value φ (0.01 mg/mL) is much smaller than those typically reported in the case of magnetic nanoparticles (0.5–5 mg/mL). This is a considerable error source for the calculation of the SAR, and therefore, in those cases in which we are only working with one microwire, we have normalized the measurements to the maximum SAR value and just focused on the evolution of SAR as a function of the analyzed parameter (glass thickness, core diameter, wire alignment, etc.).

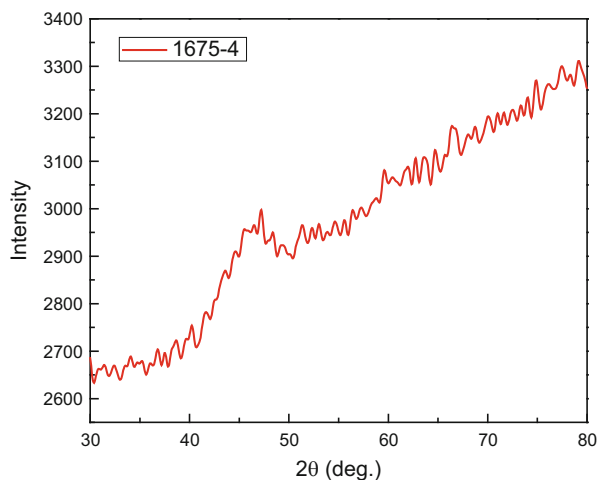
7.3 Results and Discussion

This section consists of the results of the structural characterization methods of XRD and SEM, magnetic properties of all the microwires, and their effectiveness as hyperthermia agents. The tests include discussions of the effects of different variables including metallic core diameter, glass-coating thickness, microwire number, separation, and orientation.

7.3.1 Structural Analysis

Figure 7.3 shows the XRD pattern for a 5 mm long single microwire sample of alloy number 1675-4. It can be observed that the XRD pattern exhibits only one broad peak around $2\theta = 45^\circ$, which is often known as a diffuse halo, indicating that the microwires prepared are amorphous in nature. It has been reported that the amorphous magnetic microwires are more desirable for many applications due to their good mechanical properties as compared to their crystalline counterparts [13]. In our study, the microwires used are Co-based, so their particular magnetic domains are reserved if the wires are amorphous rather than crystalline.

Fig. 7.3 XRD pattern of a glass-coated amorphous microwire 1675-4, i.e., $\text{Co}_{68}\text{B}_{15}\text{Si}_{10}\text{Mn}_7$ from 20° to 80°



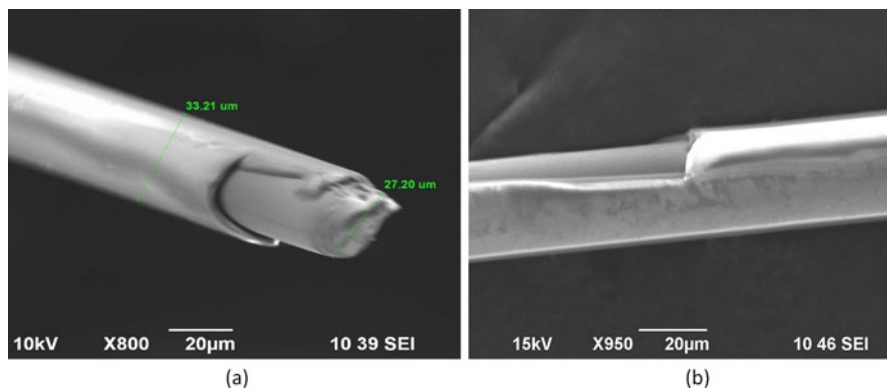


Fig. 7.4 SEM images of a glass-coated amorphous microwire 1675-4, i.e., $\text{Co}_{68}\text{B}_{15}\text{Si}_{10}\text{Mn}_7$ for two different segments (a, b)

7.3.2 Surface Morphology

Figure 7.4a, b shows the SEM images of a soft ferromagnetic amorphous glass-coated microwire for two different segments.

The SEM images taken of 1675-4 are representative of all the glass-coated microwires used in this experiment. The average diameter of the metallic core and the average thickness of the glass layer can be determined from these images. It can be seen that the entire length of the microwire has a slightly variable diameter. While the surface of the glass-coating layer is not very smooth, the surface of the metallic core is rather smooth. Therefore, we can expect these microwires to exhibit good magnetic properties. Since the magnetic property of a microwire depends sensitively on both the metallic core and the glass thickness, it is essential to investigate the effects of varying core diameter and glass thickness on the magnetic softness of the microwires studied in this work.

7.3.3 Magnetic Properties

The room temperature magnetic hysteresis $M(H)$ loops were collected for all the microwires. The wires were then split into comparison views for the tests performed, i.e., the effects of differences in thickness of either the core as shown in Fig. 7.5a or the glass coating as shown in Fig. 7.5b. It is generally observed that all microwires have negligible coercivity (H_c) and large saturation magnetization (M_s) indicative of their soft ferromagnetic characteristics. Upon closer inspection of the wires of comparative value, differences do begin to emerge about their M_s . As one can see clearly in Fig. 7.5a, 1675-4 has the largest M_s (~ 100 emu/g) and 1675-2 has the smallest M_s (~ 75 emu/g) among the four samples compared.

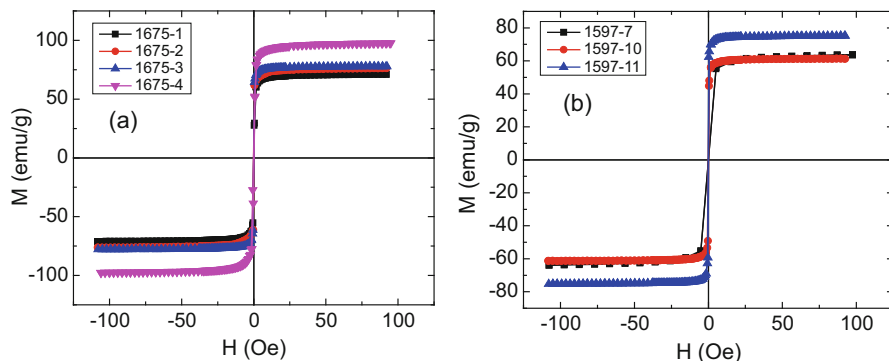


Fig. 7.5 Room temperature magnetic hysteresis $M(H)$ loops of the glass-coated amorphous microwires $\text{Co}_{68}\text{B}_{15}\text{Si}_{10}\text{Mn}_7$ and $\text{Co}_{64.61}\text{B}_{16}\text{Si}_{11}\text{Fe}_{4.97}\text{Cr}_{3.4}\text{Ni}_{0.02}$. (a) Hysteresis loops of only 1675-1, 2, 3, and 4 that vary by core diameter. (b) Hysteresis loops of only 1597-7, 10, and 11 that vary only by glass thickness

This is attributed to the increased magnetic volume of the wire as the metallic core is increased while keeping the same glass thickness. The largest value of M_s suggests in principle a better heating efficiency for the wire 1675-4, since the SAR is proportional to the M_s [3, 6].

Figure 7.5b shows the $M(H)$ loops for the wires used in the comparison of the effect of glass thickness. Once again, there is a clear outlier for M_s as the wire 1579-11 is ~ 75 emu/g while neither 1579-7 nor 1579-10 is ~ 65 emu/g. This clearly demonstrates that for wires having the same diameter of the metallic core, the M_s is larger when the glass thickness is smaller. In the literature, this effect has been attributed to internal stresses arising from the difference in the thermal expansion coefficients of metallic nucleus and glass coating [26]. Since the heating efficiency is proportional to the M_s , one can expect significant effects of the metal core diameter and glass thickness on magnetic hyperthermia response.

7.3.4 Inductive Heating Properties

Next, we have analyzed the inductive heating properties of these microwires for magnetic hyperthermia applications. In Fig. 7.6a we have plotted the heating curves for one microwire, sample 1675-4, in 1 mL of water (0.01 mg/mL) measured at different fields, and as can be observed, the heating rate appreciably increases with increasing field. We note that the relatively low temperature values reached in all these measurements (< 32 °C after 5 min), in comparison with those typically obtained in hyperthermia measurements with magnetic nanoparticles, can be explained considering the small mass of the individual microwires. Therefore, by increasing their mass or their number, the heating rate could in principle be increased to reach the desirable temperature window for therapeutic cancer treatment.

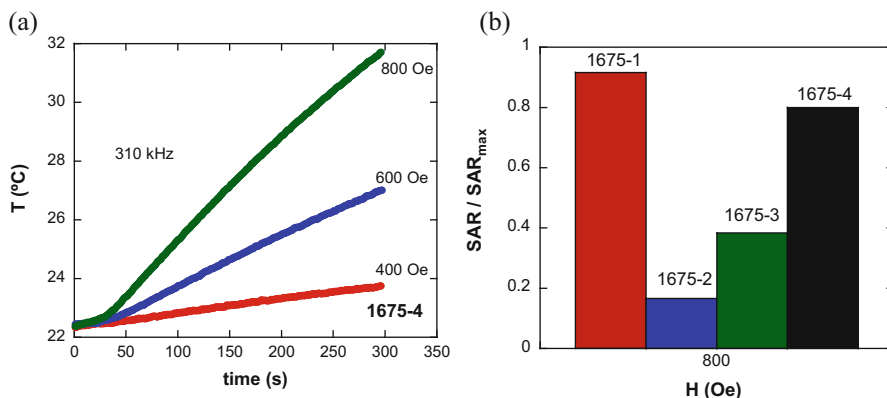


Fig. 7.6 (a) Temperature curves as a function of time at different AC fields (400–800 Oe) for sample 1675-4; (b) Normalized SAR values for 800 Oe for four samples of the same alloy (1675) with almost the same glass thickness and varying metal core diameters

Concerning the mechanism behind the heating of the microwires, as mentioned before, it could be related either to eddy current or hysteresis loss, although in principle it has been reported that in the case of soft ferromagnetic glass-coated microwires, the eddy current damping is often negligible due to the amorphous nature of the microwire presenting high electrical resistivity [12, 24].

In this study, we have analyzed the overall effects of changes in microwire dimensions using four samples of the same alloy: 1675-1, 1675-2, 1675-3, and 1675-4. All the microwires are coated with glass, which acts as an insulating barrier and enhances the biocompatibility of these materials. In Fig. 7.6b we have represented the SAR values for the four microwires that have almost the same glass thickness and varying metal core diameters. It can be observed that the SAR values of the samples 1675-1 and 1675-4 (22.8 and 25.3 μm core) are considerably larger compared to the samples 1675-2 and 1675-3 (12.9 and 15.6 μm core). In connection with the magnetization data, it is concluded that the 1675 wires with larger metal cores exhibit larger M_s , and hence larger SAR. A similar trend has been observed for the samples 1597-8 and 1597-12, with the same composition and the same glass thickness ($\sim 5.5 \mu\text{m}$), but different core diameters, 12.7 and 14.2 μm , respectively.

After this evaluation of the heating responses of the microwires, we have studied how the heating efficiency, SAR, evolves depending on the core diameter, glass thickness, and relative orientation for different applied fields (Fig. 7.7).

As observed in Fig. 7.7a, at 600 Oe, the thicker sample presents a better heating efficiency, but at higher fields, 800 Oe, the SAR values are similar, suggesting that at sufficiently high fields, the effect of the core diameter is less important than that at lower fields. Therefore, we have analyzed the effect of the glass thickness on the heating efficiency of these microwires.

In Fig. 7.7b, we have represented the SAR values for two samples, 1597-7 and 1597-10, with the same composition, the same diameter ($\sim 16.7 \mu\text{m}$), but different

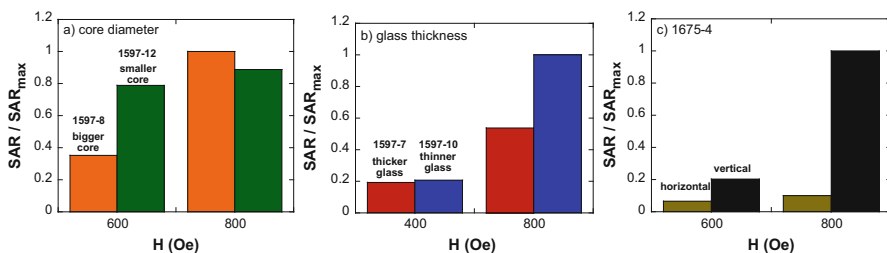
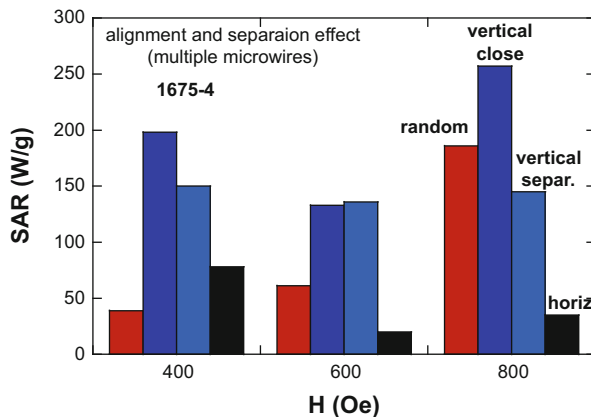


Fig. 7.7 Normalized SAR values at different fields (600 and 800 Oe) for samples with (a) the different core diameters and the same glass thickness, (b) the different glass thicknesses and the same core diameter, and (c) different orientations of the microwire with respect to the applied field

glass thicknesses, 10 and 7 μm , respectively. As can be seen in this figure, with increasing glass thickness and increasing field the SAR values tend to decrease, indicating that the glass coating partially hinders the external heat transmission from the internal metallic core. Therefore, from the point of view of hyperthermia applications, the glass coating must be kept as thin as possible to enhance the heating efficiency of the microwires. Next, we have analyzed how the alignment of the wires affects the SAR values for the sample 1675-4. In order to carry out this study, we aligned the wires in agar, both in vertical (parallel to the AC field) and horizontal (perpendicular to the AC field) directions. The agar allows us to fix the direction of the wire and make sure that the orientation does not change during the hyperthermia experiments. As observed in Fig. 7.7c, the heating efficiency is maximal when the wires are aligned in the direction of the field, and it greatly diminishes in the perpendicular direction. This is attributed to the strong shape anisotropy along the axis of the microwires. Based on this effect, we can propose a new method for controlling the heating and manipulating the inductive heating efficiency of the microwire by simply rotating the microwire by an angle ($\alpha \leq 90^\circ$) with respect to the direction of the AC applied field, while keeping a constant AC field. Instead of rotating the microwire, rotating an inductive coil about its axis to vary the direction of the AC field appears to be more efficient for practical use. Future research should thus be performed to fully exploit this novel approach.

Finally, we have measured the heating efficiency for multiple microwires (five). As we noted above, the mass of the individual microwires is too small to produce enough heating to reach the therapeutic window. Therefore, one strategy to overcome this problem is using multiple microwires for the hyperthermia treatment instead of a single microwire. In this study, we have compared how the SAR changes as a function of the orientation (vertical and horizontal) and as a function of the relative separation between the microwires. In this case, the absolute values of SAR have been given since by increasing the number of wires, the previously commented error in the SAR determination appreciably diminishes. As can be seen in Fig. 7.8, the results indicate that the heating efficiency of the microwires randomly oriented in water is lower than that of the microwires aligned in the

Fig. 7.8 SAR values for the 1675-4 samples containing five microwires in different alignments and separations



field direction, due to the effect of the shape anisotropy. It can also be observed that the heating efficiency is higher for the microwires being in direct contact than for the microwires being well separated. These results suggest that the closer the microwires, the stronger the dipolar interactions (the induced magnetostatic anisotropy), thus giving rise to an enhanced heating efficiency. The obtained SAR values are relatively high if we compare them with those typically reported for magnetic nanoparticles [27].

7.4 Concluding Remarks and Future Scope

Throughout this chapter, we have systematically demonstrated the potential of soft ferromagnetic glass-coated microwires for clinical hyperthermia applications. In particular, we have demonstrated appreciable heating rates for microwires when bundled together. We have also demonstrated the conditions that permit glass-coated microwires to perform most efficiently based on size, thickness, orientation, and distribution to develop new glass-coated microwires that balance the best aspects from each of these studies. The important results from our study are summarized below.

We have investigated the use of glass-coated microwires as an alternative to magnetic nanoparticles. With their magnetic bistability, enhanced magnetic softness, GMI effect, fast domain wall propagation, and Hopkinson effect, glass-coated microwires are a very promising alternative that does not require difficult and expensive synthesis techniques, and avoid possible biocompatibility issues and toxic effects due to accumulation in body organs. Magnetization measurements demonstrated negligible coercivity ($H_c \sim 0.2$ Oe) and high magnetization saturation ($M_s \sim 100$ emu/g) of the microwires. Additionally, we have demonstrated that single microwires show an increasing trend in heating efficiency with increased applied fields for both $\text{Co}_{64.61}\text{B}_{16}\text{Si}_{11}\text{Fe}_{4.97}\text{Cr}_{3.4}\text{Ni}_{0.02}$ and $\text{Co}_{68}\text{B}_{15}\text{Si}_{10}\text{Mn}_7$. Due to

the small mass of these glass-coated microwires, however, their SAR values are only comparable to nanoparticles when measuring multiple wires at a time.

We have studied the effects of varying levels of glass coating, varying from 6 to 10 μm in diameter, on hyperthermia efficiency of $\text{Co}_{64.61}\text{B}_{16}\text{Si}_{11}\text{Fe}_{4.97}\text{Cr}_{3.4}\text{Ni}_{0.02}$ microwires. As expected, increasing the external magnetic field from 400 to 800 Oe, the microwire with the thicker glass coat led to a decrease in SAR. 1597-7's higher SAR value demonstrates a more efficient release of heat than 1597-10. This provides some evidence that the glass coating does hinder the heat transfer between the metallic core and the surrounding environment. For biomedical applications, however, the glass-coat is important to retain the wires biocompatible. Further investigation must be done to determine the critical thickness that the glass-coat must be in order to maintain biocompatibility but still allow for efficient heat transfer. It is another controllable variable to continue to improve clinical hyperthermia optimization.

Further optimization can be accomplished by controlling the diameter of the metallic core. We have studied the influence of varying the metallic core diameter while retaining the same glass thickness in $\text{Co}_{64.61}\text{B}_{16}\text{Si}_{11}\text{Fe}_{4.97}\text{Cr}_{3.4}\text{Ni}_{0.02}$ microwires. As predicted, alloy number 1597-12, with its thicker metallic core, demonstrated higher SAR values at lower magnetic fields and approximately equal SAR values at higher magnetic fields. This indicates that a thicker microwire may be possible to implement at lower magnetic fields to achieve the same effect if higher magnetic fields are unavailable or are hazardous to the patient. Once again, however, a balance must be achieved because extremely thick microwires may result in rejection by the body, increase the difficulty in injecting the wires, or limit microwire movement to the target location.

We have also investigated the effects of orientation of the microwires, perpendicular and parallel, to the AC field for both a single microwire and for a group of five microwires. Systematically, we have shown that the vertical orientation produces far better SAR values at all magnetic fields. This is the expected result based on the microwire's domain structure. With alternating circular domains perpendicular to the domain axis, these negative magnetostrictive alloys would perform best when the applied field was not interfering with the natural domain alignment. By acting in the axis of orientation, the external magnetic field is not impeded by the internal structure. We have also determined that the closer the microwires, the greater the heating efficiency.

Having given a broad but limited study on the heating effects of amorphous soft ferromagnetic microwires, our study opens up innovative directions for further research into the hyperthermia applications of this class of microwire. Some examples are given below:

1. Our study provided insight into the difficulties in studying heat loss of single and small microwires. Therefore, future studies could limit their analysis to testing the same variables using single microwires with large magnetic cores ($>50 \mu\text{m}$) or multiple microwires where the effects of error are decreased significantly. Those studies also can expand the use of multiple microwires from five to ten or more.

2. Proper studies on matching the real-life scenarios of clinical hyperthermia should be done with glass-coated microwires. In these tests, the microwires should be tested to investigate the time it takes to reach the clinical hyperthermia temperature range, how well the temperature can be maintained, and the distribution of heat between the target location and the surrounding environment/tissue. Different alloys, different glass thicknesses, and different numbers of microwires could be tested.
3. While the Co-rich microwires were studied in this study, Fe-based microwires with appropriate compositions and dimensions could also be a competitive candidate for clinical hyperthermia applications. Suitable annealing of these Fe-based microwires could potentially improve their magnetic softness and hence inductive heating responses. Further research should thus be performed to exploit this class of microwires fully.

Acknowledgements The research was supported by the College of Arts and Science—University of South Florida Research Grant (Magnetic and hyperthermia measurements). Javier Alonso acknowledges the financial support provided through a postdoctoral fellowship from Basque Government. We thank Professors Hariharan Srikanth and Pritish Mukherjee of the University of South Florida for their useful comments and discussions. Microfir TehnologiiIndustriale (www.microwires.com) is acknowledged for providing the soft ferromagnetic glass-coated microwires for this study.

References

1. Alteri, R., Bertaut, T., Brooks, D., et al.: Cancer Facts & Figures 2015. American Cancer Society, Atlanta (2015)
2. Stewart, B., Wild, C.P.: World Cancer Report 2014. World Health Organization, Lyon (2014)
3. Ortega, D., Pankhurst, Q.A.: Magnetic hyperthermia. *Nanoscience*. **1**, 60 (2013)
4. Chertok, B., Moffat, B.A., David, A.E., et al.: Iron oxide nanoparticles as a drug delivery vehicle for MRI monitored magnetic targeting of brain tumors. *Biomaterials*. **29**, 487 (2008)
5. Colombo, M., Carregal-Romero, S., Casula, M.F., et al.: Biological applications of magnetic nanoparticles. *Chem. Soc. Rev.* **41**, 4306 (2012)
6. Périgo, E.A., Hemery, G., Sandre, O., et al.: Fundamentals and advances in magnetic hyperthermia. *Appl. Phys. Rev.* **2**, 041302 (2015)
7. Pankhurst, Q.A., Connolly, J., Jones, S.K., et al.: Applications of magnetic nanoparticles in biomedicine. *J. Phys. D: Appl. Phys.* **36**, R167 (2003)
8. Skyes, E.A., Dai, Q., Tsoi, K.M., et al.: Nanoparticle exposure in animals can be visualized in the skin and analyzed via skin biopsy. *Nat. Commun.* **5**, 3796 (2013)
9. Stauffer, P.R., Cetas, T.C., Fletcher, A.M., et al.: Observations on the use of ferromagnetic implants for inducing hyperthermia. *IEEE Trans. Biomed. Eng.* **31**, 76 (1984)
10. Zuchini, R., Tsai, H.W., Chen, C.Y., et al.: Electromagnetic thermotherapy using fine needles for hepatoma treatment. *Eur. J. Surg. Oncol.* **37**, 604 (2011)
11. Vázquez, M.: Soft magnetic wires. *Physica B*. **299**, 302 (2001)
12. Zhukov, A., Zhukova, V.: *Magnetic Properties and Applications of Ferromagnetic Microwires with Amorphous and Nanocrystalline Structure*. Hauppauge, New York (2009)
13. Phan, M.H., Peng, H.X.: Giant magnetoimpedance materials: fundamentals and applications. *Prog. Mater. Sci.* **53**, 323 (2008)

14. Hudak, R., Varga, R., Hudak, J., et al.: Influence of fixation on magnetic properties of glass-coated magnetic microwires for biomedical applications. *IEEE Trans. Magn.* **51**, 5200104 (2015)
15. Banobre-Lopez, M., Teijeiro, M., Rivas, J.: Magnetic nanoparticle-based hyperthermia for cancer treatment. *Rep. Prac. Oncol. Radiother.* **18**, 397 (2013)
16. Jordan, A., Wust, P., Fahling, H., et al.: Inductive heating of ferrimagnetic particles and magnetic fluids—physical evaluation of their potential for hyperthermia. *Int. J. Hyperth.* **9**, 51 (1993)
17. Gilchrist, R.K., Shorey, W.D., Hanselman, R.C., et al.: Effects of electromagnetic heating on internal viscera: a preliminary to the treatment of human tumors. *Ann. Surg.* **161**, 890 (1965)
18. Lucia, O.: Induction heating and its applications: past developments, current technology, and future challenges. *IEEE Trans. Ind. Electron.* **61**, 2509 (2014)
19. Figuerola, A., Di Corato, R., Manna, L., et al.: From iron oxide nanoparticles towards advanced iron-based inorganic materials designed for biomedical applications. *Pharmacol. Res.* **62**, 126 (2010)
20. Gómez-Polo, C., Larumbe, S., Pérez-Landazabal, J.I., et al.: Magnetic induction heating of FeCr nanocrystalline alloys. *J. Magn. Magn. Mater.* **324**, 1897 (2012)
21. Gómez-Polo, C., Larumbe, S., Pérez-Landazabal, J.I., et al.: Analysis of heating effects (magnetic hyperthermia) in FeCrSiBCuNb amorphous and nanocrystalline wires. *J. Appl. Phys.* **111**, 07A314 (2012)
22. Qin, F.X., Peng, H.X.: Ferromagnetic microwires enabled multifunctional composite materials. *Prog. Mater. Sci.* **58**, 183 (2013)
23. Colosimo, P., Chen, A., Devkota, J., Srikanth, H., Phan, M.H., et al.: Sensing RF and microwave energy with fiber Bragg grating heating via soft ferromagnetic glass-coated microwires. *Sens. Actuators A* **210**, 25 (2014)
24. Varga, R.: Magnetization processes in glass-coated microwires with positive magnetostriction. *Acta Phys. Slov.* **62**, 411 (2012)
25. Ulitovsky, A.V.: Micro-technology in design of electric devices. *Leningrad.* **7**, 6 (1951)
26. Chizhik, A., Zhukova, V.: Magneto-optical and magnetic studies of Co-rich glass-covered microwires. *Phys. Res. Int.* **2012**, 690793 (2012)
27. Kolhatkar, A.G., Jamison, A.C., Litvinov, D., et al.: Tuning the magnetic properties of nanoparticles. *Int. J. Mol. Sci.* **14**, 15977 (2013)